Tuning the endothelial response: differential release of exocytic cargos from Weibel-Palade Bodies.

Thomas D. Nightingale[1], Jessica J. McCormack[2], William Grimes[2, 3], Christopher Robinson[1], Mafalda Lopes da Silva[2], Ian J. White[2], Andrew Vaughan[2], Louise P. Cramer[2] and Daniel F. Cutler[2‡]

[1]Centre for Microvascular Research, William Harvey Research Institute, Barts and the London School of Medicine and Dentistry, Queen Mary University of London, Charterhouse Square, London EC1M6BQ, UK.
[2]MRC Laboratory of Molecular Cell Biology, University College London, Gower Street, London, WC1E6BT, UK.
[3]Imaging Informatics Division, Bioinformatics Institute, 30 Biopolis Street, Singapore.

[‡]Corresponding author

Email d.cutler@ucl.ac.uk
Address: MRC Laboratory for Molecular Cell Biology, Cell Biology Unit and Department of Cell and Developmental Biology, UCL, Gower Street, London. WC1E6BT
Phone: +44 (20) 7679 7808

Running title: Differential release from Weibel-Palade Bodies

Essentials

- Endothelial activation initiates multiple processes, including haemostasis and inflammation
- The molecules that contribute to these processes are co-stored in secretory granules.
- How can the cells control release of granule content to allow differentiated responses?
- Selected agonists recruit an exocytosis-linked actin ring to boost release of a subset of cargo.

Abstract

Background: Endothelial cells harbour specialised storage organelles, Weibel-Palade Bodies (WPBs). Exocytosis of WPB content into the vascular lumen initiates primary haemostasis, mediated by Von Willebrands factor (VWF) and inflammation, mediated by several proteins including P-selectin. During full fusion, secretion of this large haemostatic protein and smaller pro-inflammatory proteins are thought to be inextricably linked.

Objective: To determine if secretagogue-dependent differential release of WPB cargo occurs, and whether this is mediated by the formation of an actomyosin ring during exocytosis.

Methods: We used VWF string analysis, leukocyte rolling assays, ELISA, spinning disk confocal microscopy, high-throughput confocal microscopy and inhibitor and siRNA treatments to demonstrate the existence of cellular machinery that allows differential release of WPB cargo proteins.

Results: Inhibition of the actomyosin ring differentially effects two processes regulated by WPB exocytosis; it perturbs VWF string formation but has no effect on leukocyte rolling. The efficiency of ring recruitment correlates with VWF release; the ratio of release of VWF to small cargoes decreases when ring recruitment is inhibited. The recruitment of the actin ring is time-dependent; fusion events occurring directly after stimulation are less likely to initiate haemostasis than later events, and is activated by PKC isoforms.

Conclusions: Secretagogues differentially recruit the actomyosin ring, thus demonstrating one mechanism by which the pro-thrombotic effect of endothelial activation can be modulated. This potentially limits thrombosis whilst permitting a normal inflammatory response. These results have implications for the assessment of WPB fusion, cargo-content release and the treatment of patients with von Willebrand disease.

Keywords: Von Willebrand Factor, Weibel-Palade Bodies, Exocytosis, Hemostasis, Inflammation

Introduction

A rapid response to vascular injury or infection minimises blood loss and spread of pathogens. Endothelial rod-shaped storage organelles called Weibel-Palade bodies (WPB) harbour multiple pre-made, pro-inflammatory and pro-haemostatic proteins[1-3], including the leukocyte receptor P-selectin, the pro-haemostatic glycoprotein Von Willebrands factor (VWF), pro-inflammatory cytokines, and agents that control tonicity[4]. Some cargos are up-regulated after endothelial activation including IL-8[5, 6] and angiopoeitin-2[7]. Within minutes of secretagogue stimulation WPBs undergo exocytosis[8, 9], releasing their content into the blood which initiates haemostasis and leukocyte recruitment[2].

Release of VWF and P-selectin have distinct functional consequences. VWF multimers are stored in multi-concatamer coiled proteinacious tubules, together with their cleaved pro-peptides[10]. Upon exocytosis, the tubules unfurl into long protein strings, that recruit platelets even at non-pathological shear[11, 12].

VWF mutations, or defective cellular machinery cause incorrect processing and can underlie bleeding disorders[13]. Animal models of or patients with low VWF exhibit a decreased incidence of atherosclerosis[14]. Conversely excess ultra-high molecular weight VWF in the bloodstream (due to induced or genetic absence of the VWF-cleaving metalloprotease ADAMSTS13), results in the microvascular occlusions[15] of thrombotic thrombocytopenic purpura, and patients with elevated plasma VWF have an increased risk of cardiac events[14, 16] and stroke[17]. VWF is thus a key factor in cardiovascular disease. P-selectin is a leukocyte receptor that mediates initial rolling of leukocytes on the vascular endothelium[18-20]. Loss or inappropriate clustering of P-selectin at the endothelial cell surface results in immunodeficiency due to a failure to recruit leukocytes[20, 21].

Being co-stored, parallel release at exocytosis of VWF and smaller components such as P-selectin should be obligatory. However, there is evidence of differential release of VWF [22-24]. At low extracellular pH unfolding of VWF is prevented such that only small soluble components are released[22], whilst in lingering kiss fusion, comprising about 10% of fusion events after strong histamine stimulation[23], only cargo proteins ≤40kDa are released. However, neither of these mechanisms enables differential release of VWF vs P-selectin and therefore the segregation of inflammatory and haemostatic effects. Furthermore, no molecular machinery providing physiological control of VWF release has been identified.

Recent research has uncovered machinery controlling the efficiency of VWF release from WPBs [9, 25, 26]. If differentially recruited by agonists, this would potentially promote regulated release of pro-haemostatic VWF whilst not altering release of smaller pro-inflammatory components. Such "differential release", a novel layer of regulation, could limit potentially dangerous thrombosis whilst allowing a normal inflammatory response. We have used multiple *in vitro* assays to show that recruitment of an actomyosin ring allows differential release of cargo following stimulation by numerous physiologically-relevant secretagogues. We also describe protein kinase-C as upstream machinery that modulates its recruitment.

Methods

Cell culture and nucleofection

HUVECs were cultured as described previously[27]. GFP-VWF[28] was from J. Voorberg and J.A. Van Mourik (Sanquin Research Laboratory, Amsterdam, Netherlands). P-sel.Lum–mCherry was previously described [9] Lifeact-GFP[29] was from B. Baum (University College London, UK). GFP-tagged PKCα and PKCβ were gifts from A. Poole (University of Bristol, UK), GFP-tagged PKCδ and PKCε were from P. Parker (Francis Crick Institute, London, UK). DNA (1–5 μg) was nucleofected using program U-001 (Lonza). Cells were typically assayed 24 h post-transfection.

Immunofluorescence

This was detailed previously[9].

Secretion assay and ELISA

HUVECs were incubated with 1 μM CCE, 25 μM blebbistatin (Sigma-Aldrich) for 5–15 min before determining VWF or pro-peptide release in the presence or absence of 100 ng/ml PMA (Sigma-Aldrich), 100 μM histamine or 100 μM histamine/10 μM adrenalin/ 100 μM IBMX and/or the relevant drug for 30 min. VWF secretion assay and ELISAs have been described previously[30][31]. For VWF pro-peptide secretion an ELISA kit (Mast Group Ltd) was used according to the manufacturer's instructions.

Exocytic site labelling assay

Exocytic site labelling was performed using a modified method from Knop and Gerke, 2002 [32]. Confluent cells grown on 96 well plates (Nunc) for two days were washed in pre-warmed release medium (M199 with 0.2% BSA and 10mM HEPES), and where necessary incubated with CCE or blebbistatin as for secretion assays. Cells were incubated for 2-20 minutes in the presence of rabbit anti-VWF and either unstimulated, or stimulated with PMA (6.25-100ng/ml), histamine (100 μM), thrombin (1U/μl), VEGF (40ng/ml), Forskolin (10μM), ATP (100μM), or adrenalin (10 μM)/IBMX (100 μM), either alone or in combination, in release medium. Cells were incubated with wheat germ agglutinin (Life Technologies) for two minutes on ice or fixed immediately in 4% paraformaldehyde, permeabilised with 0.2% Triton X-100 in PBS and incubated with mouse anti-VE-cadherin (BD biosciences) or with secondary antibodies conjugated to Alexa Fluor 488- or 647-nm and Hoescht 33342.

High-throughput image acquisition and segmentation.

Cells were cultured, fixed and stained in 96-well plates then imaged with the Opera high-content screening (PerkinElmer) confocal microscope using a 40× air objective lens (NA 0.6). Datasets comprise 864 images (nine fields of view per well), approximately 10,000 cells. Analysis used Python2.7, with the scikit-image library[33]. Image noise was reduced by Gaussian blurring, then a binary mask was created using a threshold value from Moment-preserving thresholding[34]. Adjacent sites were split using the marker-based watershed flooding algorithm. Segmented objects beneath the resolution limit of the optical system were removed. Finally, morphometric measurements were taken. Segmentation was validated by comparison to a set of manually-annotated images. Data analysis was conducted in the R programming language version 3.2[35].

Western blotting

This was carried out as described previously[9].

Live-cell imaging

Nucleofected cells stimulated with PMA, histamine, or histamine/adrenalin/IBMX were visualized as detailed previously using a 100× oil immersion lens (NA 1.4) on a spinning-disk system (UltraVIEW VoX; PerkinElmer)[9].

VWF string analysis and quantification

String assays were carried out as described previously[9].

Rolling assay and quantification

HUVECs prepared as for string assays were placed on the stage of an Axiovert 200M microscope at 37°C, connected to a syringe pump, and HBSS media perfused for 2 minutes at a constant wall shear stress 0.07Pa (0.7 dyne/cm^3). HUVECs were then either perfused with HBSS alone or stimulated with histamine/adrenaline/IBMX in the presence or absence of CCE (0.25 μM) for five minutes before being perfused with THP-1 cells (0.5 x 10^6/ml) in HBSS in the presence or absence of secretagogue. Videos were recorded using a Rolera Bolt CMOS camera (QImaging) using MicroManager software. Videos were analysed using ImageJ. Interacting THP-1 cells were defined as those seen to pause on the endothelial monolayer and counted manually.

Cell surface biotinylation assay

This was carried out as described previously[21].

Results

We and others demonstrated that VWF release is boosted by a contractile actomyosin ring forming around the fused WPB to squeeze out content [9, 25, 26], but whether this boost affects platelet and leukocyte recruitment to endothelial cells was undetermined. We first analysed the effect of actomyosin ring inhibition on VWF string formation (Fig. 1A-C). HUVECs grown in flow chambers were briefly treated with a low dose (thus without an effect on cell viability or adherence) of the actin depolymerising drug cytochalasin E (CCE) which binds to the barbed end of the actin chain[36]. A cocktail (to stimulate both calcium and cAMP-mediated pathways of WPB exocytosis) of histamine, adrenalin and 3-isobutyl-1-methyl xanthine (IBMX) was used to stimulate WPB

exocytosis and the length of resulting strings was analysed. In cells treated with CCE the formation of long strings was significantly reduced (Fig. 1A-C). To determine if leukocyte recruitment is also reduced we monitored rolling in the presence or absence of CCE. We saw no significant difference in the frequency of rolling leukocytes following drug treatment (Fig. 1D; video 1-3). Thus in a controlled system, inhibition of the actomyosin ring differentially affects inflammatory vs. haemostatic functioning. We hypothesise that the regulation of VWF secretion by the actomyosin ring is a secretagogue-dependent way to bias the endothelial response to be more or less haemostatic.

VWF is by far the largest WPB cargo protein, likely requiring the most physical force for efficient release, potentially explaining why control of the actin ring specifically affects haemostatic responses. Similarly, smaller pro-inflammatory content should be less affected by actin ring inhibition (Fig. 2A-B). Further, to provide physiological regulation, different secretagogues should differentially utilise the actin ring. To test this we used three secretagogues which activate different downstream signalling pathways[4]; PMA, histamine, and histamine/adrenalin/IBMX. To determine the effect of content size on its efficiency of release, we compared secretion of VWF (large cargo) (Fig. 2Ci) with VWF pro-peptide (small cargo) (Fig. 2Cii). The pro-peptide is necessarily co-packaged in equi-molar amounts with VWF, thus providing exact ratiometric data. Further, the pro-peptide is increasingly used clinically to determine VWF clearance [37], thus evidence of its differential release is of intrinsic interest. Whilst PMA and histamine/adrenalin/IBMX were similarly effective at exocytosing both large and small content, histamine releases the large cargo

VWF much less efficiently than PMA. This was most clearly apparent when presented as the ratio of VWF/pro-peptide release to give a measure of the secretion efficiency of large vs small cargo (Fig. 2Ciii).

To determine if this difference in efficiency depends on the actomyosin machinery we used CCE to inhibit actin polymerisation and blebbistatin[38] to block non-muscle myosin II contraction (Fig. 2D). CCE completely inhibits ring formation whilst blebbistatin reduces the rate of ring contraction. As predicted, efficient release of VWF following PMA stimulation requires the actomyosin ring; these inhibitors reduced VWF release (Fig. 2Di). Conversely, release of the smaller VWF pro-peptide is essentially actin ring-independent (Fig. 2Dii). The ratio of VWF to pro-peptide release following PMA stimulation is 0.4±0.05, whilst in cells which cannot recruit the ring, efficiency of release falls to 0.2±0.04 (Fig. 2Diii). Interestingly, PMA-stimulated cells in which the actin ring is inhibited behave similarly to histamine-stimulated cells in terms of efficiency of VWF release. This data shows that the actomyosin ring provides a means for secretagogue-dependent control of VWF release without affecting smaller cargo.

We next addressed whether the actomyosin ring influenced the delivery of integral membrane proteins to the cell surface from WPBs. We stimulated HUVECs with different secretagogues and monitored P-selectin appearance on the plasma membrane (Fig. 3A & C). The most efficient delivery to the plasma membrane occurred following PMA stimulation, whereas histamine and histamine/adrenalin/IBMX behave similarly. The delivery of P-selectin to the cell surface in response to PMA was partially dependent on the actomyosin ring as

283 both blebbistatin and CCE reduced cell surface levels (Fig. 3B & D). The reason
284 for this is unclear but might reflect VWF/P-selectin binding, retaining P-selectin
285 within the WPB after fusion [39]. Consistent with this, as reported, P-selectin is
286 enriched along VWF strings [40] and at exocytic sites post-exocytosis (Fig. S1,
287 Fig. 3E). Alternatively, the partial inhibition could reflect a steric hindrance of the
288 extracellular domain of P-selectin as it exits the fusion pore; P-selectin mobility
289 is limited in mature WPBs [41]. Therefore, the delivery of larger integral
290 membrane proteins can be influenced by inhibition of the actin ring although not
291 enough to inhibit function (Fig 1D).
292
293 To directly determine the extent and kinetics of actin ring recruitment, we
294 monitored actin ring recruitment in live cells [9]. We monitored the loss of
295 mcherry-Pselectin.lum (marking WPB fusion) and the recruitment of lifeact-GFP
296 (tracking ring assembly) and found (Fig. 4A) that approximately ≈15% of
297 histamine-stimulated fusion events, ≈40% of histamine/adrenalin/IBMX-
298 stimulated events and ≈65% of PMA-stimulated events recruit the ring.
299 Additionally, the probability of ring recruitment increases over time (Fig. 4B).
300 Immediately following stimulation (0-50s), and irrespective of secretagogue, the
301 likelihood of recruitment is low. For PMA and histamine/adrenalin/IBMX-
302 stimulated cells this is followed by increased ring recruitment (50-200s) (68%
303 and 69% of events are actin-positive in PMA and histamine/adrenalin/IBMX-
304 stimulated cells respectively over 100-600s). In histamine-stimulated cells the
305 majority of events are actomyosin ring-independent, although the percentage of
306 actin-positive events increases over time, until every event recruited a ring
307 (though few events occur at these later times). Therefore time-dependent

phenomena are likely required for ring recruitment, presumably including both signalling and recruitment of machinery.

We next sought to determine whether recruitment of the actomyosin ring following stimulation by the many established WPB secretagogues [4, 42] both alone and in combination is a major feature of exocytosis. We developed an assay for determination of the size of the fusion site. This assay takes advantage of information obtained previously using correlative light and electron microscopy and scanning electron microscopy showing that levels of exocytosed, antibody - accessible VWF is dependent on the actomyosin ring[9]. We added anti-VWF antibody to the media to retain VWF at exocytic sites (and prevent string formation) [32, 43] to analyse exocytic site formation in thousands of cells. We hypothesised that more efficient release mediated by the actin ring is likely to result in bigger sites (Fig. 5B), and developed an automated segmentation protocol to acquire a set of morphological measurements for each site from 72 fields of view (950-1200 cells) analysed per condition (Fig. 5A).

This approach is unbiased, automated, and highly sensitive, as shown by our analyses revealing that the number of sites increased in response to increased PMA in a dose-dependent manner (Fig. S2Aa), without change to the site area (Fig. S2Ab). Thus, even at a high density, segmentation of individual sites is not compromised. Histamine elicits a rapid response, typically complete by 10 minutes post-stimulation, whereas PMA produces a more linear release of VWF [44]. Importantly, these biochemical dynamics were replicated in our assay, which is sensitive enough to distinguish differences in the number of exocytic

sites over discrete two-minute periods (Fig. 5C). To verify the assay could differentiate ring-dependent and independent exocytic events we monitored the number (Fig. 5D) and area of sites (Fig. 5E) and noted that sites segmented from stimulated cells were significantly larger than those from unstimulated cells, and that PMA-stimulated cells produce larger sites than histamine-stimulated cells – correlating with actin ring recruitment. We therefore analysed changes in histamine and PMA-stimulated cells treated with blebbistatin and CCE to determine the effect of actin ring inhibition on the proportion of large exocytic sites (classified as those greater than 2μm^2) (Fig. 5G, Fig. S2B). CCE treatment specifically reduces the proportion of larger exocytic sites following both PMA and histamine stimulation, whilst blebbistatin, as expected, had little effect (as it slows rather than completely inhibits actomyosin ring contraction). This effect was greatest in PMA-stimulated cells (Fig. 5G, Fig. S2B). Together this validates a new, sensitive, high-throughput method of monitoring VWF exocytic sites suitable for screening secretagogues for their ability to recruit the actomyosin ring.

We then surveyed different secretagogues for their use of the actomyosin ring. By determining the number (Fig. 6A, Fig. S3A & B) and size of exocytic sites (Fig. 6B-D, Fig. S3C & D) following stimulation with different secretagogues in isolation or combination, we found significant differences in actin ring recruitment (Fig. 6C & D, Fig. S3C-F). Whilst, thrombin relies minimally on the actin ring for release of VWF, PMA, VEGF, histamine/adrenalin/IBMX and forskolin are strong ring recruiters (correlating with ours and others' findings [9, 25]). We also find that actin ring recruitment can be enhanced via addition of

some, but not all, Calcium or cAMP-raising agents (Fig. 6 & Fig S3), which is consistent with our earlier ELISA data. Our approach provides large quantitative datasets to reveal actin ring-dependence for a range of secretagogues and indicates for the first time that endothelial cells, by responding to physiological cues, have the capability to tune the release of cargo content.

We next sought the upstream machinery required for actin ring recruitment. Actin-dependent exocytic structures occur in the cortical granules of *Xenopus* oocytes, the zymogen granules of the pancreatic and parotid acinar and the lamellar bodies of type II pneumocytes[45]. Some of these granules utilise protein kinase C (PKC) isoforms to recruit an actin ring[46, 47]. Given this, and that PMA (an activator of classical and non-classical PKC isoforms) recruits the actin ring most efficiently, we analysed the role of PKC in ring recruitment.

PKCα, PKCδ, PKCε, PKCη and PKCζ are expressed in HUVECs [48]. Live-cell imaging of individual fusion events using mCherry-P-selectinLum as a marker of fusion and various human GFP-tagged versions of PKC showed recruitment of PKCα and PKCδ on the actin ring (Fig. 7A & B) but not epsilon, nor beta (not endogenously expressed; data not shown) suggesting specific recruitment. Recruitment of PKC prior to the actin ring is consistent with a role upstream of or during initiation of ring recruitment. (Fig. S4). To assess the function of these isoforms in VWF release from PMA-stimulated cells we depleted either PKCα or PKCδ (Fig. 7C) and monitored VWF release by ELISA. PKCα but not PKCδ knockdown had a marked effect (Fig. 7D).

Finally, we monitored the effect of an inhibitor of PKCα on VWF secretion (Fig. 7E). Predictably, PKCα inhibition had the strongest effect on PMA-stimulated release, a lesser effect on histamine/adrenalin/IBMX-stimulated release and no effect on histamine-stimulated release (Fig. 7E, Fig. S5A). We also noted some reduction in the number of exocytic sites seen in PMA-stimulated cells, with a lesser effect on histamine or histamine/adrenalin/IBMX (Fig. S5B & C). An additional role for PKC in exocytosis is thus possible alongside the formation of the actomyosin ring.

Discussion

We present here evidence for the differential release of WPB cargo that we speculate can allow the separation of haemostatic and inflammatory responses. We find that different secretagogues are differentially effective at recruiting an actomyosin ring to WPBs at exocytosis, and that recruitment of this ring correlates with the release of the largest WPB cargo protein, VWF. Ultimately this represents a new layer of control to facilitate greater regulation over the outcome of endothelial activation.

We firstly demonstrated that two functions ascribed to WPB cargo content can be differentially regulated. We used an *in vitro* flow chamber to separate effects on leukocyte adhesion from VWF string formation in endothelial cells treated with a low dose of the actin poison CCE. Recruitment of the actomyosin ring affected VWF string formation (and therefore the efficiency of platelet recruitment) (Fig. 1A-C) but not leukocyte recruitment (Fig. 1D).

To determine if this effect reflects size-specific control of the release of WPB cargo, we monitored release of equimolar co-packaged VWF multimers (large protein) versus VWF pro-peptide (small protein) in parallel. We found that only the release of VWF was differentially evoked by secretagogues, and that this correlated with the recruitment of an actin ring (Fig. 2). Stimulation with histamine alone was not efficient at releasing VWF relative to the pro-peptide, whereas PMA or histamine/adrenalin/IBMX were much more efficient (Fig. 2C). Similar reductions in efficiency followed perturbation of actomyosin ring function at PMA stimulation plus blebbistatin or CCE (Fig. 2D); squeezing by the actin ring is more important for larger cargoes than small ones, and this can explain some of the differences revealed by functional assays. The greater effects of CCE than blebbistatin likely reflects the fact that CCE inhibits ring formation whilst blebbistatin only slows the rate of its contraction.

Leukocyte rolling following secretagogue stimulation is initiated by P-selectin [19, 20] clustered at the cell surface by the WPB co-cargo CD63 [21]. CD63 readily transfers to the plasma membrane even in situations where VWF release is inhibited, including release at low pH [22] or during lingering kiss fusion [23]. Surface biotinylation demonstrated that P-selectin traffic to the cell surface is partially actomyosin ring-dependent (Fig. 3) although we see no difference in leukocyte rolling following actomyosin ring inhibition (Fig. 1D). Direct interactions with VWF (also suggested by imaging Fig. S1) may explain this effect [39]. The clustering effects of CD63, or a simple excess of receptor may help to mitigate the differences seen in P-selectin recruitment to the cell surface.

Directly imaging ring recruitment (Fig. 4) to determine which secretagogues recruit the ring to the greatest extent corroborated our ELISA results. Notably, we also identified a time-dependence to ring recruitment, with later exocytic events with all tested stimuli much more likely to recruit the ring. This intriguing time course suggests that downstream signalling is required both to recruit the actin ring and to localise associated cellular machinery.

The most efficient actin ring recruitment (and therefore VWF release) occurs when multiple secretagogues are used (Fig. 2 & 4). We utilised a new high-throughput approach to monitor a range of secretagogues (Fig. 5, 6 & S2). Assaying thousands of exocytic sites from thousands of cells, this approach affords excellent temporal sensitivity and statistical significance. *In vivo* the endothelium is likely stimulated by multiple secretagogues; histamine activation is accompanied by at least some adrenalin (resting levels are 0.31nM [49]). Identifying the signalling pathways downstream of secretagogue activation is complex, as many intersect. One of the strongest ring-promoting agents is the non-physiological DAG analogue PMA, suggesting PKC involvement (most likely PKCα) (Fig. 7). Since PKCα can be activated directly by both DAG and Calcium [50] or indirectly via cAMP-dependent agonists and EPAC (exchange proteins directly activated by cAMP isoform) [51, 52] PKC activation could feasibly occur downstream of any of the ring-recruiting agonists that we, and others, have identified. The cAMP-raising secretagogues forskolin and adrenalin have previously been identified by others [25] as stimulating actin ring recruitment. Here we find that addition of adrenalin/IBMX to the Calcium-dependent secretagogue histamine significantly enhances ring recruitment, suggesting

458 activation of cAMP may be an important route to ring recruitment. Interestingly,
459 thrombin, which is largely actin ring independent, can inhibit cAMP production,
460 potentially explaining why this is a poor ring recruiter [53]. However, it is likely
461 that other, as-yet-unidentified pathways independent of PKCα are also involved
462 in ring recruitment. Histamine alone is able to recruit the actin ring, despite the
463 fact that its mode of action is thought to be PKC-independent [48]. Although
464 PKCα acts in ring recruitment, VEGF is also effective at recruiting the actin ring
465 and acts via PKCδ (and VWF release is not inhibited by inhibition of PKCα in
466 VEGF-stimulated cells) [48], thus roles for additional PKC isoforms are possible.
467
468 VWF release is not completely actin ring-dependent, as CCE treatment does not
469 abolish it, and secretagogues that do not utilise the ring still expel VWF, albeit at
470 a lower efficiency (Fig. 2-6) as measured by pro-peptide vs VWF release. Thus
471 cargo expulsion may also be driven by water entry, changes in ionic fluxes or pH
472 [54]. We have also found protracted actin ring formation and slower release of
473 content at lowered external pH (data not shown). Other large acidified granules
474 with viscous content including lamellar bodies, pancreatic and parotid acinar
475 zymogen granules all require extra machinery to drive release [45], indicating
476 that charge is not always the sole and most efficient driving force. Other large
477 granules may also exhibit differential recruitment of actin rings and therefore
478 differential release of content.
479
480 Our research complements recent research confirming that VWF release is
481 boosted by an actomyosin ring[25, 26]. However, there are differences in the
482 findings: We concluded that rings form *de novo* after fusion [9], whereas Han *et*

al report actin remodelling before fusion from a pre-existing framework. We also differ on whether WPB localisation is generally affected by Myosin II inhibition[9, 26]. The different conclusions might reflect which cell surface was imaged (apical versus basal) or spinning disk versus custom microscopy [9, 25]. A role for some actin nucleation yet remains a possibility.

Differential release has previously been proposed, based on the presence of multiple pools of WPB [24]. While additional cargos can be added to WPB including IL-8[5, 6] and angiopoeitin-2[7] we have no evidence to suggest the ring can be differentially recruited to distinct WPB containing different cargos; this would require cytoplasmic machinery detecting cargo stored internally in WPB.

Our results support the clinical use of VWF pro-peptide monitoring, perhaps immediately after agonist treatment, where needed. We also note that DDAVP, the secretagogue most commonly used to treat VWD patients, is cAMP-dependent [55] and perhaps this is one reason why it is an effective therapeutic choice.

In conclusion, these data provide evidence for an additional level of functional control of WPBs, concluding that endothelial cells may tune the haemostatic response via the recruitment of an actomyosin ring.

<u>Addendum</u>

JJM and TDN equally made the greatest contributions to this paper; both invented novel assays, designed and carried out experiments, analysed data and wrote the manuscript; CR, WG and MLS, designed and carried out experiments and contributed to the writing of this paper, IJW and AV provided technical expertise and analysed data, LPC and DFC designed research, analysed data and wrote the paper.

Disclosure of Conflict of Interest

T. D. Nightingale was funded by a Medical Research Council project grant MR/M019179/1 and a British Heart Foundation project grant (PG/15/72/31732). J.J. McCormack and D.F. Cutler were funded by an MRC programme grant MC_UU_12018/2. I.J. White was funded by MRC LMCB core. W. Grimes was supported partly by the Biomedical Research Council of A*STAR (Agency for Science, Technology and Research), Singapore, partly by the MRC LMCB. C. Robinson was funded by a BHF project grant (PG/15/72/31732). M. Lopes da Silva reports grants from MRC during the conduct of the study; and grants from MRC outside the submitted work. The other authors state that they have no conflict of interest.

532

533

534 References

535 1 Metcalf DJ, Nightingale TD, Zenner HL, Lui-Roberts WW, Cutler DF.
536 Formation and function of Weibel-Palade bodies. *J Cell Sci*. 2008; **121**: 19-27.
537 121/1/19 [pii]
538 10.1242/jcs.03494.
539 2 Nightingale T, Cutler D. The secretion of von Willebrand factor from
540 endothelial cells; an increasingly complicated story. *Journal of thrombosis and*
541 *haemostasis : JTH*. 2013; **11 Suppl 1**: 192-201. 10.1111/jth.12225.
542 3 Valentijn KM, Sadler JE, Valentijn JA, Voorberg J, Eikenboom J. Functional
543 architecture of Weibel-Palade bodies. *Blood*. 2011; **117**: 5033-43. blood-2010-
544 09-267492 [pii]
545 10.1182/blood-2010-09-267492.
546 4 Rondaij MG, Bierings R, Kragt A, van Mourik JA, Voorberg J. Dynamics and
547 plasticity of Weibel-Palade bodies in endothelial cells. *Arteriosclerosis,*
548 *thrombosis, and vascular biology*. 2006; **26**: 1002-7.
549 5 Utgaard JO, Jahnsen FL, Bakka A, Brandtzaeg P, Haraldsen G. Rapid
550 secretion of prestored interleukin 8 from Weibel-Palade bodies of microvascular
551 endothelial cells. *The Journal of experimental medicine*. 1998; **188**: 1751-6.
552 6 Wolff B, Burns AR, Middleton J, Rot A. Endothelial cell "memory" of
553 inflammatory stimulation: human venular endothelial cells store interleukin 8 in
554 Weibel-Palade bodies. *The Journal of experimental medicine*. 1998; **188**: 1757-62.
555 7 Fiedler U, Scharpfenecker M, Koidl S, Hegen A, Grunow V, Schmidt JM, Kriz
556 W, Thurston G, Augustin HG. The Tie-2 ligand angiopoietin-2 is stored in and
557 rapidly released upon stimulation from endothelial cell Weibel-Palade bodies.
558 *Blood*. 2004; **103**: 4150-6. 10.1182/blood-2003-10-3685.
559 8 Erent M, Meli A, Moisoi N, Babich V, Hannah MJ, Skehel P, Knipe L,
560 Zupancic G, Ogden D, Carter T. Rate, extent and concentration dependence of
561 histamine-evoked Weibel-Palade body exocytosis determined from individual
562 fusion events in human endothelial cells. *J Physiol*. 2007; **583**: 195-212.
563 9 Nightingale TD, White IJ, Doyle EL, Turmaine M, Harrison-Lavoie KJ,
564 Webb KF, Cramer LP, Cutler DF. Actomyosin II contractility expels von
565 Willebrand factor from Weibel-Palade bodies during exocytosis. *The Journal of*
566 *cell biology*. 2011; **194**: 613-29. jcb.201011119 [pii]
567 10.1083/jcb.201011119.
568 10 Springer TA. von Willebrand factor, Jedi knight of the bloodstream. *Blood*.
569 2014; **124**: 1412-25. 10.1182/blood-2014-05-378638.
570 11 De Ceunynck K, De Meyer SF, Vanhoorelbeke K. Unwinding the von
571 Willebrand factor strings puzzle. *Blood*. 2013; **121**: 270-7. blood-2012-07-
572 442285 [pii]
573 10.1182/blood-2012-07-442285.
574 12 Dong JF, Moake JL, Nolasco L, Bernardo A, Arceneaux W, Shrimpton CN,
575 Schade AJ, McIntire LV, Fujikawa K, Lopez JA. ADAMTS-13 rapidly cleaves newly
576 secreted ultralarge von Willebrand factor multimers on the endothelial surface
577 under flowing conditions. *Blood*. 2002; **100**: 4033-9.

13 James PD, Lillicrap D. The molecular characterization of von Willebrand disease: good in parts. *British journal of haematology*. 2013; **161**: 166-76. 10.1111/bjh.12249.
14 van Galen KP, Tuinenburg A, Smeets EM, Schutgens RE. Von Willebrand factor deficiency and atherosclerosis. *Blood reviews*. 2012; **26**: 189-96. 10.1016/j.blre.2012.05.002.
15 Zheng XL. ADAMTS13, TTP and Beyond. *Hereditary genetics : current research*. 2013; **2**: e104. 10.4172/2161-1041.1000e104.
16 Jin SY, Tohyama J, Bauer RC, Cao NN, Rader DJ, Zheng XL. Genetic ablation of Adamts13 gene dramatically accelerates the formation of early atherosclerosis in a murine model. *Arteriosclerosis, thrombosis, and vascular biology*. 2012; **32**: 1817-23. 10.1161/ATVBAHA.112.247262.
17 Wieberdink RG, van Schie MC, Koudstaal PJ, Hofman A, Witteman JC, de Maat MP, Leebeek FW, Breteler MM. High von Willebrand factor levels increase the risk of stroke: the Rotterdam study. *Stroke; a journal of cerebral circulation*. 2010; **41**: 2151-6. 10.1161/STROKEAHA.110.586289.
18 Bonfanti R, Furie BC, Furie B, Wagner DD. PADGEM (GMP140) is a component of Weibel-Palade bodies of human endothelial cells. *Blood*. 1989; **73**: 1109-12.
19 McEver RP, Beckstead JH, Moore KL, Marshall-Carlson L, Bainton DF. GMP-140, a platelet alpha-granule membrane protein, is also synthesized by vascular endothelial cells and is localized in Weibel-Palade bodies. *The Journal of clinical investigation*. 1989; **84**: 92-9. 10.1172/JCI114175.
20 Mayadas TN, Johnson RC, Rayburn H, Hynes RO, Wagner DD. Leukocyte rolling and extravasation are severely compromised in P selectin-deficient mice. *Cell*. 1993; **74**: 541-54.
21 Doyle EL, Ridger V, Ferraro F, Turmaine M, Saftig P, Cutler DF. CD63 is an essential cofactor to leukocyte recruitment by endothelial P-selectin. *Blood*. 2011; **118**: 4265-73. blood-2010-11-321489 [pii] 10.1182/blood-2010-11-321489.
22 Babich V, Knipe L, Hewlett L, Meli A, Dempster J, Hannah MJ, Carter T. Differential effect of extracellular acidosis on the release and dispersal of soluble and membrane proteins secreted from the Weibel-Palade body. *The Journal of biological chemistry*. 2009; **284**: 12459-68.
23 Babich V, Meli A, Knipe L, Dempster JE, Skehel P, Hannah MJ, Carter T. Selective release of molecules from Weibel-Palade bodies during a lingering kiss. *Blood*. 2008; **111**: 5282-90.
24 Cleator JH, Zhu WQ, Vaughan DE, Hamm HE. Differential regulation of endothelial exocytosis of P-selectin and von Willebrand factor by protease-activated receptors and cAMP. *Blood*. 2006; **107**: 2736-44. 10.1182/blood-2004-07-2698.
25 Han X, Li P, Yang Z, Huang X, Wei G, Sun Y, Kang X, Hu X, Deng Q, Chen L, He A, Huo Y, Li D, Betzig E, Luo J. Zyxin regulates endothelial von Willebrand factor secretion by reorganizing actin filaments around exocytic granules. *Nat Commun*. 2017; **8**: 14639. 10.1038/ncomms14639.
26 Li P, Wei G, Cao Y, Deng Q, Han X, Huang X, Huo Y, He Y, Chen L, Luo J. Myosin IIa is critical for cAMP-mediated endothelial secretion of von Willebrand factor. *Blood*. 2017. 10.1182/blood-2017-08-802140.

27 Michaux G, Abbitt KB, Collinson LM, Haberichter SL, Norman KE, Cutler DF. The physiological function of von Willebrand's factor depends on its tubular storage in endothelial Weibel-Palade bodies. *Developmental cell*. 2006; **10**: 223-32. 10.1016/j.devcel.2005.12.012.
28 Romani de Wit T, Rondaij MG, Hordijk PL, Voorberg J, van Mourik JA. Real-time imaging of the dynamics and secretory behavior of Weibel-Palade bodies. *Arteriosclerosis, thrombosis, and vascular biology*. 2003; **23**: 755-61. 10.1161/01.ATV.0000069847.72001.E8.
29 Riedl J, Crevenna AH, Kessenbrock K, Yu JH, Neukirchen D, Bista M, Bradke F, Jenne D, Holak TA, Werb Z, Sixt M, Wedlich-Soldner R. Lifeact: a versatile marker to visualize F-actin. *Nature methods*. 2008; **5**: 605-7. 10.1038/nmeth.1220.
30 Lui-Roberts WW, Collinson LM, Hewlett LJ, Michaux G, Cutler DF. An AP-1/clathrin coat plays a novel and essential role in forming the Weibel-Palade bodies of endothelial cells. *The Journal of cell biology*. 2005; **170**: 627-36.
31 Blagoveshchenskaya AD, Hannah MJ, Allen S, Cutler DF. Selective and signal-dependent recruitment of membrane proteins to secretory granules formed by heterologously expressed von Willebrand factor. *Molecular biology of the cell*. 2002; **13**: 1582-93. 10.1091/mbc.01-09-0462.
32 Knop M, Gerke V. Ca2+ -regulated secretion of tissue-type plasminogen activator and von Willebrand factor in human endothelial cells. *Biochim Biophys Acta*. 2002; **1600**: 162-7.
33 van der Walt S, Schonberger JL, Nunez-Iglesias J, Boulogne F, Warner JD, Yager N, Gouillart E, Yu T, scikit-image c. scikit-image: image processing in Python. *PeerJ*. 2014; **2**: e453. 10.7717/peerj.453.
34 Tsai W. Moment-preserving thresholding: a new approach. In: O'Gorman LaK, Rangachar, ed. *Document image analysis* 44-60: IEEE Computer Society Press Los Alamitos, CA, USA, 1995.
35 Team RDC. R: A Language and Environment for Statistical Computing. www.R-project.org/: the R Foundation for Statistical Computing, 2011.
36 Forscher P, Smith SJ. Actions of cytochalasins on the organization of actin filaments and microtubules in a neuronal growth cone. *The Journal of cell biology*. 1988; **107**: 1505-16.
37 Sanders YV, Groeneveld D, Meijer K, Fijnvandraat K, Cnossen MH, van der Bom JG, Coppens M, de Meris J, Laros-van Gorkom BA, Mauser-Bunschoten EP, Leebeek FW, Eikenboom J, Wi Nsg. von Willebrand factor propeptide and the phenotypic classification of von Willebrand disease. *Blood*. 2015; **125**: 3006-13. 10.1182/blood-2014-09-603241.
38 Straight AF, Cheung A, Limouze J, Chen I, Westwood NJ, Sellers JR, Mitchison TJ. Dissecting temporal and spatial control of cytokinesis with a myosin II Inhibitor. *Science*. 2003; **299**: 1743-7. 10.1126/science.1081412.
39 Michaux G, Pullen TJ, Haberichter SL, Cutler DF. P-selectin binds to the D'-D3 domains of von Willebrand factor in Weibel-Palade bodies. *Blood*. 2006; **107**: 3922-4. 10.1182/blood-2005-09-3635.
40 Padilla A, Moake JL, Bernardo A, Ball C, Wang Y, Arya M, Nolasco L, Turner N, Berndt MC, Anvari B, Lopez JA, Dong JF. P-selectin anchors newly released ultralarge von Willebrand factor multimers to the endothelial cell surface. *Blood*. 2004; **103**: 2150-6. 10.1182/blood-2003-08-2956.

41 Kiskin NI, Hellen N, Babich V, Hewlett L, Knipe L, Hannah MJ, Carter T. Protein mobilities and P-selectin storage in Weibel-Palade bodies. *J Cell Sci*. 2010; **123**: 2964-75. 10.1242/jcs.073593.
42 McCormack JJ, Lopes da Silva M, Ferraro F, Patella F, Cutler DF. Weibel-Palade bodies at a glance. *J Cell Sci*. 2017; **130**: 3611-7. 10.1242/jcs.208033.
43 Valentijn KM, van Driel LF, Mourik MJ, Hendriks GJ, Arends TJ, Koster AJ, Valentijn JA. Multigranular exocytosis of Weibel-Palade bodies in vascular endothelial cells. *Blood*. 2010; **116**: 1807-16. blood-2010-03-274209 [pii] 10.1182/blood-2010-03-274209.
44 Michaux G, Hewlett LJ, Messenger SL, Goodeve AC, Peake IR, Daly ME, Cutler DF. Analysis of intracellular storage and regulated secretion of 3 von Willebrand disease-causing variants of von Willebrand factor. *Blood*. 2003; **102**: 2452-8. 10.1182/blood-2003-02-0599.
45 Nightingale TD, Cutler DF, Cramer LP. Actin coats and rings promote regulated exocytosis. *Trends Cell Biol*. 2012; **22**: 329-37. S0962-8924(12)00051-7 [pii] 10.1016/j.tcb.2012.03.003.
46 Miklavc P, Wittekindt OH, Felder E, Dietl P. Ca2+-dependent actin coating of lamellar bodies after exocytotic fusion: a prerequisite for content release or kiss-and-run. *Annals of the New York Academy of Sciences*. 2009; **1152**: 43-52. 10.1111/j.1749-6632.2008.03989.x.
47 Yu HY, Bement WM. Control of local actin assembly by membrane fusion-dependent compartment mixing. *Nature cell biology*. 2007; **9**: 149-59. 10.1038/ncb1527.
48 Lorenzi O, Frieden M, Villemin P, Fournier M, Foti M, Vischer UM. Protein kinase C-delta mediates von Willebrand factor secretion from endothelial cells in response to vascular endothelial growth factor (VEGF) but not histamine. *Journal of thrombosis and haemostasis : JTH*. 2008; **6**: 1962-9. 10.1111/j.1538-7836.2008.03138.x.
49 Jabbour G, Lemoine-Morel S, Casazza GA, Hala Y, Moussa E, Zouhal H. Catecholamine response to exercise in obese, overweight, and lean adolescent boys. *Medicine and science in sports and exercise*. 2011; **43**: 408-15. 10.1249/MSS.0b013e3181f1bef3.
50 Cho W. Membrane targeting by C1 and C2 domains. *The Journal of biological chemistry*. 2001; **276**: 32407-10. 10.1074/jbc.R100007200.
51 Khaliulin I, Bond M, James AF, Dyar Z, Amini R, Johnson JL, Suleiman MS. Functional and cardioprotective effects of simultaneous and individual activation of protein kinase A and Epac. *Br J Pharmacol*. 2017; **174**: 438-53. 10.1111/bph.13709.
52 Yang W, Mei FC, Cheng X. EPAC1 regulates endothelial annexin A2 cell surface translocation and plasminogen activation. *FASEB J*. 2017. 10.1096/fj.201701027R.
53 Aslam M, Tanislav C, Troidl C, Schulz R, Hamm C, Gunduz D. cAMP controls the restoration of endothelial barrier function after thrombin-induced hyperpermeability via Rac1 activation. *Physiol Rep*. 2014; **2**. 10.14814/phy2.12175.
54 Conte IL, Cookson E, Hellen N, Bierings R, Mashanov G, Carter T. Is there more than one way to unpack a Weibel-Palade body? *Blood*. 2015; **126**: 2165-7. 10.1182/blood-2015-08-664961.

55 Kaufmann JE, Oksche A, Wollheim CB, Gunther G, Rosenthal W, Vischer UM. Vasopressin-induced von Willebrand factor secretion from endothelial cells involves V2 receptors and cAMP. *The Journal of clinical investigation*. 2000; **106**: 107-16. 10.1172/JCI9516.

Figure Legends

Figure. 1 **The actomyosin ring increases the efficiency of VWF string formation but has little effect on leukocyte rolling**

HUVECs stimulated under flow with histamine (100 μM)/adrenalin (10 μM)/IBMX (100 μM) in the presence or absence of 0.25μM cytochalasin E (CCE) and fixed for string length analysis (A-C) or perfused with THP-1 leukocytes for rolling analysis (D) (N=3). (A-B) HUVECs were fixed and stained for VWF before imaging on a confocal microscope, pictures shown are tile scans of 10 fields of view. The whole image (i) and with the boxed area magnified (ii) are shown with a filter added to improve contrast. Scale bar 50 μm (C) The lengths of vWF strings was quantified from three independent experiments (Control; N=13 images, 1346 strings, CCE; N=14 images, 1364 strings). The percentage of strings less than 25μm, between 25-50μm and longer than 50μm was calculated per image and SEM shown. (D) The number of interacting THP-1 leukocytes/min was determined from movies. Each point represents the total number of interacting leukocytes per one minute movie, with up to two movies acquired per experiment from stimulated cells. Error bars represent SD. Statistical significance assessed using Mann-Whitney test (C) and 1-way ANOVA with Dunnet's multiple comparison test (D). * $P \leq 0.05$.

Figure. 2 **Different secretagogues release VWF and VWF pro-peptide with differing efficiencies in a manner that is dependent on the actomyosin ring**

(A) HUVECs were stimulated with 100 ng/ml PMA for 5 min and fixed using a procedure optimal for the actin cytoskeleton, co-stained for VWF (red) and phalloidin (green), and imaged on a confocal microscope. Maximum intensity projections shown. Boxed regions are shown magnified. Bar 10 μm. (B) Schematic of WPB exocytosis in the presence or absence of an actomyosin ring. Small cargo release is ring-independent while VWF release is more efficient in the presence of the ring. (C) Quantification of PMA (100 ng/ml), histamine (100 μM) or histamine (100 μM)/adrenalin (10 μM)/IBMX (100 μM)-stimulated (Ci) VWF or (Cii) pro-peptide secretion, (n=6-9), error bars=SEM. (Ciii) ratio of stimulated VWF:propeptide release. Boxes represent 25^{th}-75^{th} percentiles, whiskers represent minimum and maximum values. (D) Quantification of PMA (100 ng/ml)-stimulated (Di) VWF or (Dii) pro-peptide secretion in the presence or absence of 25 μM blebbistatin or 1 μM cytochalasin E, (n=4), error bars=SEM. (Diii) ratio of stimulated VWF:propeptide release. Error bars=SEM. Statistical significance assessed using T-Test with Welch's correction (Ci-ii and Di-ii) and Ratio T-test (Ciii and Diii). * $P \leq 0.05$, ** $P \leq 0.01$ and *** $P \leq 0.001$.

Figure. 3 **Release of P-selectin from WPB for recruitment to the plasma membrane is partially ring dependent.**

The proportion of cell surface to total P-selectin levels was determined by surface biotinylation and neutravidin pulldown following stimulation with PMA (100 ng/ml) (A-B), histamine (100 μM) or histamine (100 μM)/adrenalin (10 μM)/IBMX (100 μM) (A) or following PMA stimulation or in the presence or

absence of 25 μM blebbistatin or 1 μM CCE (B). Quantification of western blots shown (C) PMA n=11, his n=3, HAI n=6, (D) n=12. (C-D) Error bars=SEM. Statistical significance assessed using T-Test with Welch's correction (C-D). * P≤0.05, ** P≤0.01 (E) Schematic of WPB exocytosis in the presence or absence of an actomyosin ring. NMMII=non-muscle myosin II.

Figure. 4 **Actin ring recruitment is secretagogue and time dependent.**
HUVECs were nucleofected with mCherry-PselectinLum domain and lifeactGFP and imaged with a spinning-disk confocal microscope in the presence of 100 ng/ml PMA (n=9), 100 μM histamine (n=7) or 100 μM histamine/10 μM adrenalin/100 μM IBMX (n=8). Z stacks were acquired at a spacing of 0.5 μm every 5 s for 10 min. (A) The frequency of fusion events with (positive +ve) or without an actin ring (negative -ve) at each time-point is plotted. (B) The percentage of actin ring-positive (+ve) or negative events (-ve) compared to the total number of events is plotted.

Figure 5. **High-throughput analysis of exocytic events.**
(A) HUVECs were unstimulated or stimulated with 100ng/μl PMA for 10 minutes followed by staining for external VWF, plasma membrane with wheat germ agglutinin (WGA) and the nucleus (DAPI). Nine fields of view were acquired per well, and eight wells imaged per condition. External VWF was segmented using a custom-designed program. Boxed areas on the VWF channel are shown inverted and at higher magnification as examples of segmented sites typically acquired from unstimulated and PMA-stimulated cells. Scale bar 20μm. (B) Schematic of external antibody labelling protocol to differentiate between actomyosin-

dependent and independent exocytosis. NMMII=non-muscle myosin II. (C) HUVECs stimulated with either histamine (100 μM) or PMA (100 ng/ml) were fixed following 2-20 minutes of stimulation. The number of segmented external exocytic sites was calculated for each well (the sum of nine fields of view) for each time point and mean and standard error plotted (N=8 wells). A representative experiment is shown from N=4 independent experiments. (D & E) HUVECs were stimulated for 10 min with PMA (100 ng/ml) or histamine (100 μM) or left unstimulated. The mean number of exocytic sites per cell per well (D) (N=8 wells, a representative experiment is shown from N=3 independent experiments) and the median area per site (E) (N=9-16 independent experiments) is shown. Bars represent SEM. (F & G) HUVEC were untreated or pre-treated with blebbistatin (25 μM) or CCE (1 μM) for 15 min before stimulation with histamine and PMA. The mean number of sites per cell (F) (N=3 independent experiments) and the proportion of sites with area greater than 2 μm^2 (G) (N=8 wells, a representative experiment from N=3 independent experiments is shown). Boxes represent 25^{th}-75^{th} percentiles, whiskers represent minimum and maximum values. Statistical significance was assessed using 2-way ANOVA with sidak's multiple comparison test (C & G), or 1-way ANOVA with Tukey's multiple comparison test (E). * P≤0.05, ** P≤0.01, *** P≤0.001, ****≤0.0001.

Figure 6. **Analysis of actin ring function with a variety of secretagogues.** HUVECs were treated with or without 1μM CCE before being stimulated with 100ng/μl PMA, 100μM histamine, 1U/ml thrombin, 10μM adrenalin/100 μM IBMX 100 μM histamine/10μM adrenalin/100μM IBMX, 10μm forskolin/100 μM

824 IBMX, or 40ng/ml VEGF for 10 minutes, followed by staining for external VWF
825 and the nucleus. Nine fields of view were acquired per well, and eight wells
826 imaged per condition. Data from representative experiments shown (A-C) (N=3)
827 and the mean of 3-7 experiments (D). (A) Mean number of exocytic sites per cell
828 per well following secretagogue stimulation. Bars are SEM. (N=8 wells). (B)
829 Cumulative frequency graph shows the distributions of the area of exocytic sites.
830 (C) The mean proportion of exocytic VWF-positive sites with area greater than
831 2μm^2 was calculated following stimulation with various secretagogues with and
832 without CCE (1μM). Boxes represent 25th-75th percentiles, whiskers represent
833 minimum and maximum values. N=8 wells. (D) The mean proportion of exocytic
834 sites with area greater than 2μm^2 following stimulation with a number of
835 secretagogues in the presence of CCE normalised to the mean proportion of large
836 sites in control samples. Mean value is derived from the n=8 wells per
837 experiment (n=3-7). Statistical significance assessed between stimulated and
838 unstimulated distributions using Two sample Kolmogorov-Smirnov test (B), 2-
839 way ANOVA with Sidak's multiple comparison test (C) and 1-way ANOVA with
840 Dunnet's multiple comparisons test (D) * P≤0.05, ** P≤0.005, *** P≤0.001, ****
841 P≤0.0001, @ P≤10^{-15}.
842
843 Figure. 7 **The role of protein kinase C isoforms in actin ring recruitment and**
844 **VWF secretion.**
845 (A, B) HUVECs were nucleofected with PKCαGFP (A) or PKCδGFP (B) and
846 stimulated for 5 min with 100 ng/ml PMA, fixed in formaldehyde with a
847 procedure optimal for the actin cytoskeleton, co-stained for VWF (blue) and
848 phalloidin (red) and imaged on a confocal microscope. Image shown is a

maximum intensity projection, boxed regions are shown magnified. Bar 10 μm. (C, D) HUVECs were nucleofected with 2 rounds of 200 pmol siRNA against PKCα, δ or both isoforms together and either (C) the samples were prepared for western blot or (D) VWF secretion monitored. (E) HUVEC were treated with 1μM GÖ6976 and then stimulated with PMA (100ng/ml), histamine (100μM) or a combination of histamine (100μM), adrenalin (10μM) and IBMX (100μM). VWF secretion was monitored and results are shown normalised to the uninhibited sample. The PKC inhibitor has the greatest effect on PMA-stimulated release and a lesser effect on hist/ad/IBMX. n=4, error bars=SEM. Statistical significance assessed using T-Test with Welch's correction. * $P<0.05$ and ** $P<0.01$.

Video 1. **Rolling analysis of untreated endothelial cells.**

Unstimulated HUVECs were perfused with THP-1 leukocytes.

Video 2. **Rolling analysis of endothelial cells stimulated with Histamine and Adrenalin.**

HUVECs were stimulated under flow with Histamine (100 μM)/Adrenalin (10 μM)/IBMX (100 μM) and perfused with THP-1 leukocytes.

Video 3. **Rolling analysis untreated endothelial cells.**

HUVECs were stimulated under flow with Histamine (100 μM)/Adrenalin (10 μM)/IBMX (100 μM) in the presence of 0.25μM cytochalasin E (CCE) and perfused with THP-1 leukocytes.

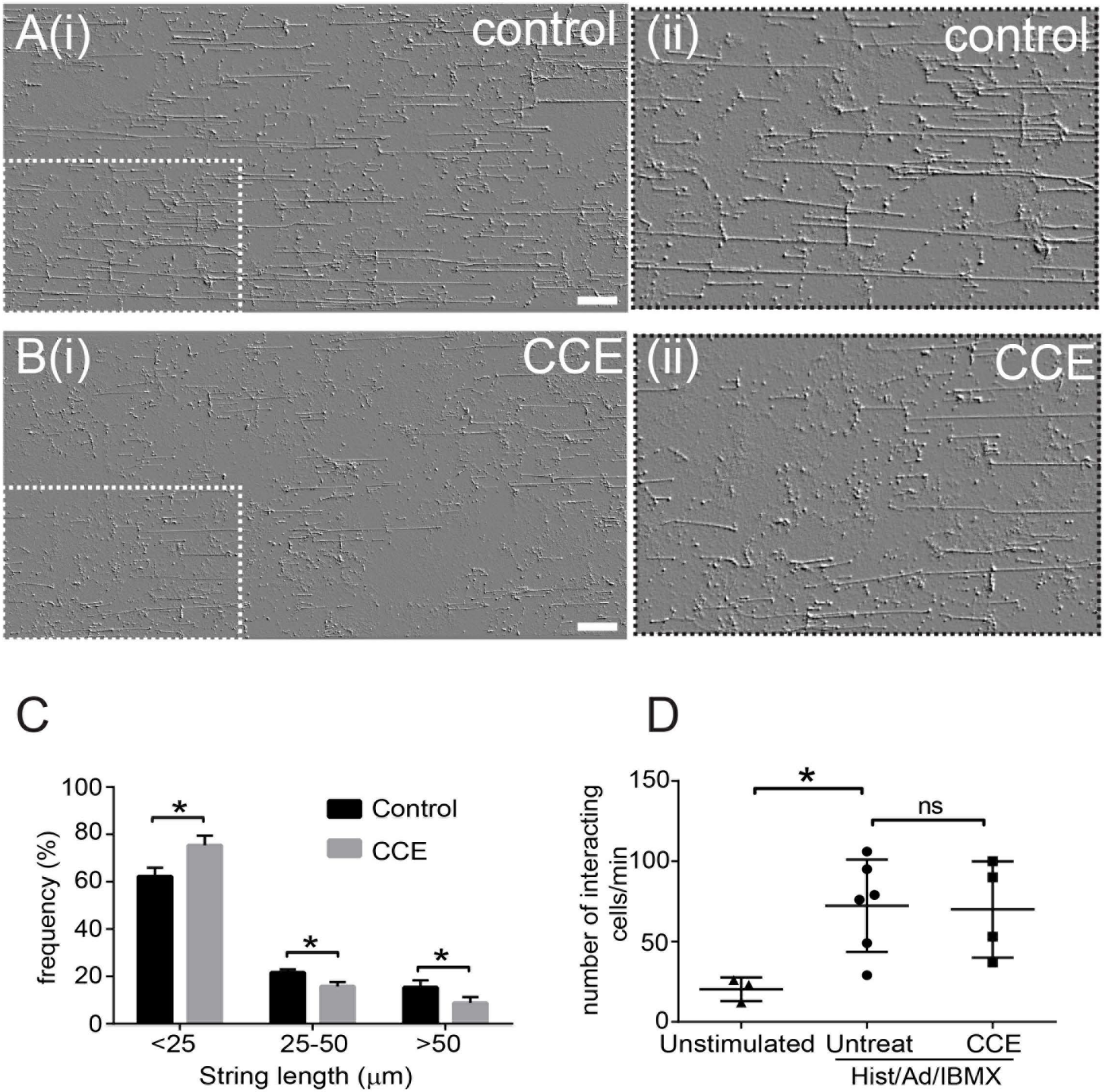
A(i)
control
(ii)
control
B(i)
CCE
(ii)
CCE
C
100
80
60
40
20
0
frequency (%)
*
*
*
Control
CCE
<25
25-50
>50
String length (μm)
D
150
100
50
0
number of interacting cells/min
*
ns
Unstimulated
Untreat
CCE
Hist/Ad/IBMX

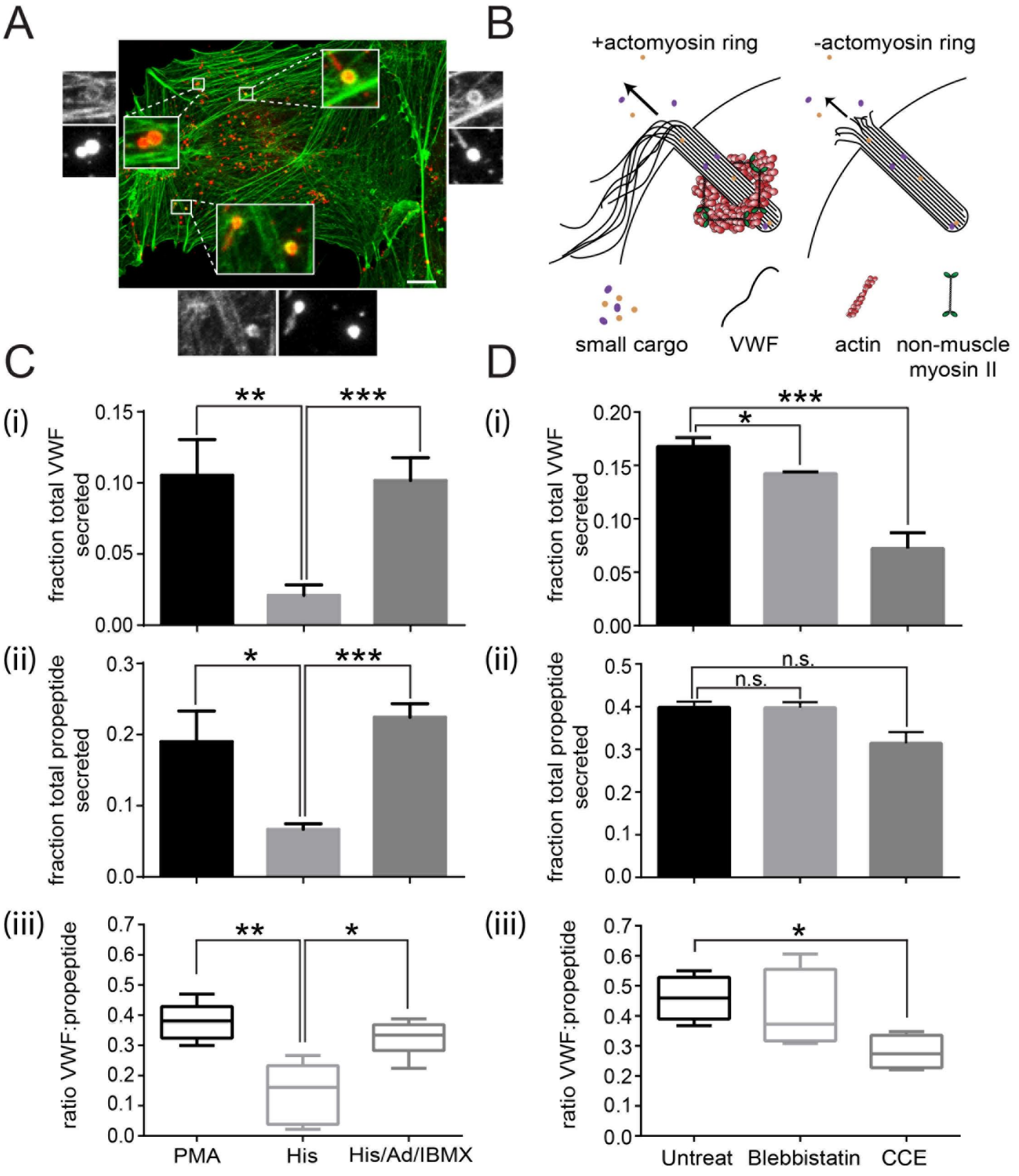
A
B
+actomyosin ring
-actomyosin ring
small cargo
VWF
actin
non-muscle myosin II
C
D
(i)
(ii)
(iii)
fraction total VWF secreted
fraction total propeptide secreted
ratio VWF:propeptide
**
***
*
n.s.
PMA
His
His/Ad/IBMX
Untreat
Blebbistatin
CCE

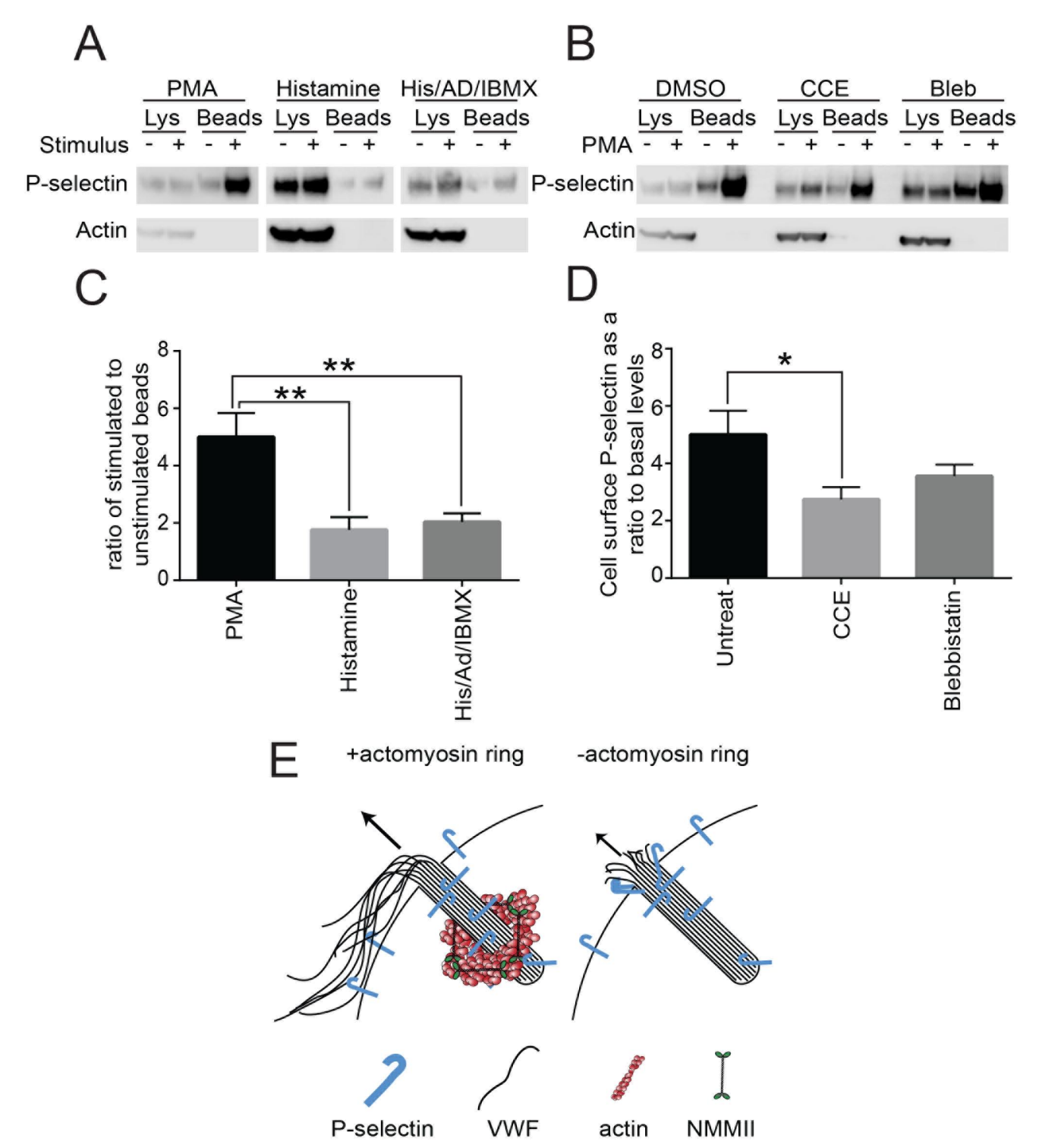
A
PMA
Histamine
His/AD/IBMX
Lys
Beads
Stimulus
- + - + - + - + - + - +
P-selectin
Actin
B
DMSO
CCE
Bleb
Lys
Beads
PMA
- + - + - + - + - + - +
P-selectin
Actin
C
ratio of stimulated to unstimulated beads
0
2
4
6
8
**
**
PMA
Histamine
His/Ad/IBMX
D
Cell surface P-selectin as a ratio to basal levels
0
2
4
6
8
*
Untreat
CCE
Blebbistatin
E
+actomyosin ring
-actomyosin ring
P-selectin
VWF
actin
NMMII

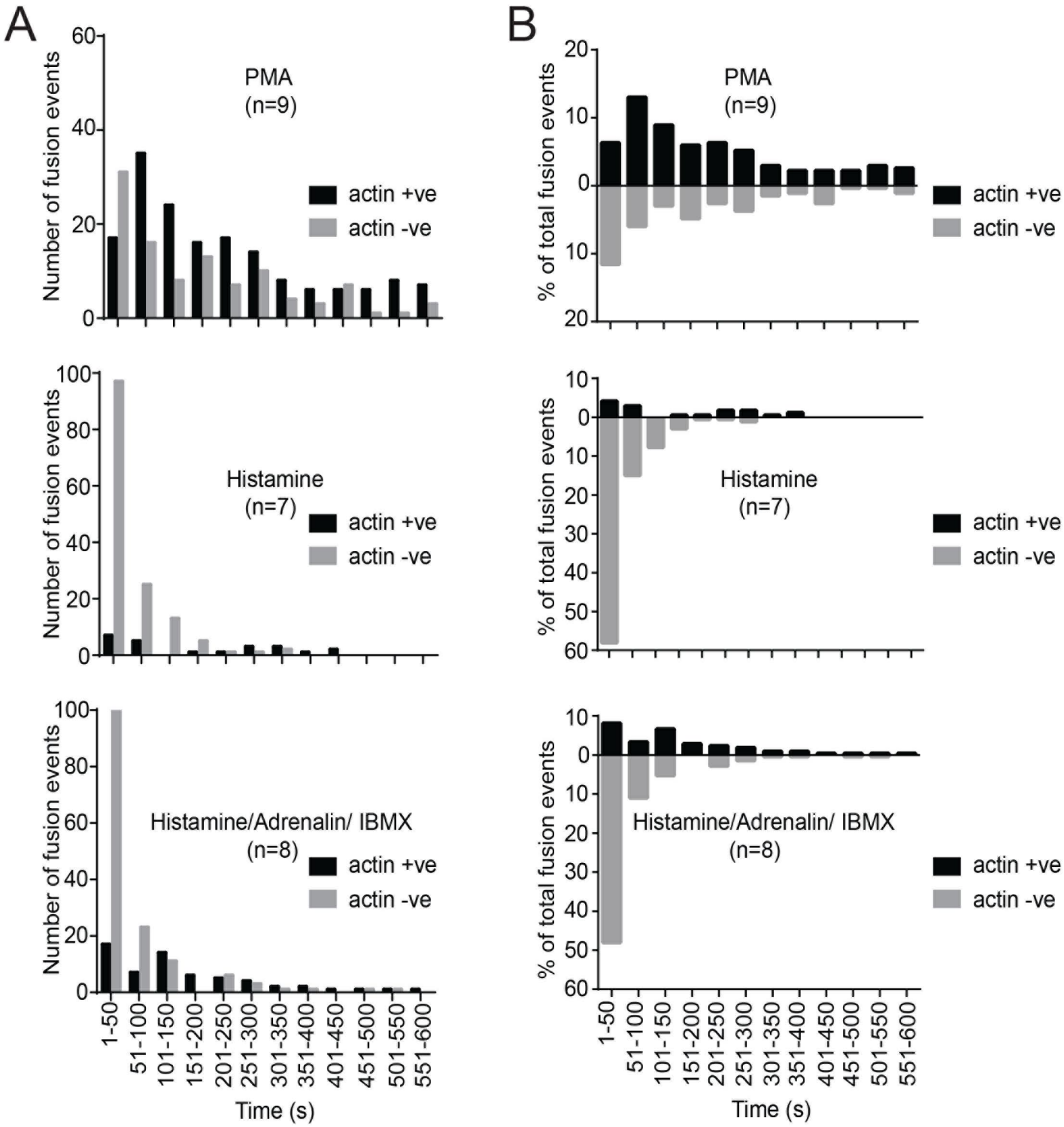
A
B
PMA
(n=9)
Histamine
(n=7)
Histamine/Adrenalin/ IBMX
(n=8)
Number of fusion events
% of total fusion events
actin +ve
actin -ve
Time (s)
1-50
51-100
101-150
151-200
201-250
251-300
301-350
351-400
401-450
451-500
501-550
551-600

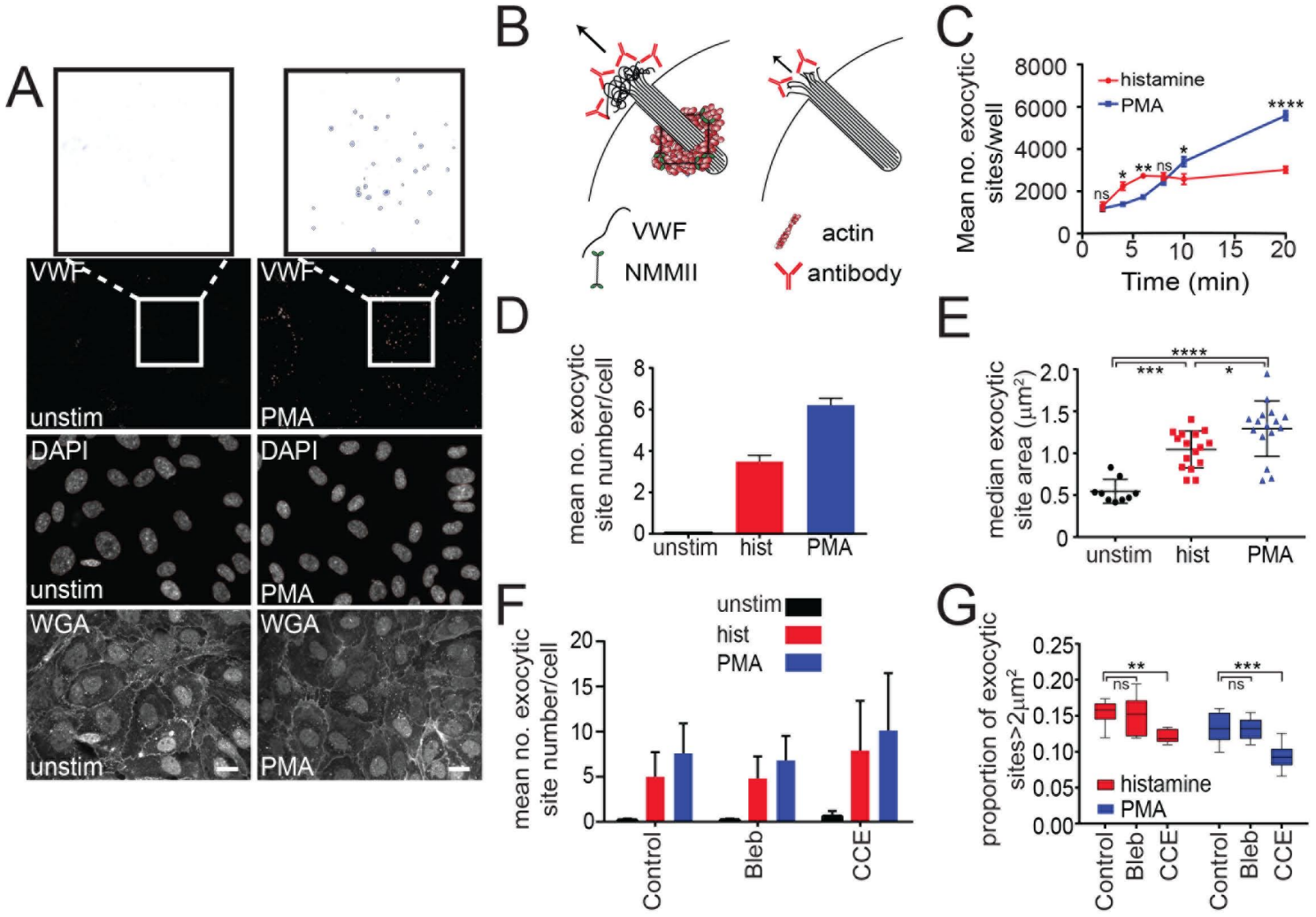
A
VWF
unstim
VWF
PMA
DAPI
unstim
DAPI
PMA
WGA
unstim
WGA
PMA
B
VWF
NMMII
actin
antibody
C
Mean no. exocytic sites/well
8000
6000
4000
2000
0
histamine
PMA
ns
*
**
ns
*
****
0
5
10
15
20
Time (min)
D
mean no. exocytic site number/cell
8
6
4
2
0
unstim
hist
PMA
E
median exocytic site area (μm²)
2.0
1.5
1.0
0.5
0
****
***
*
unstim
hist
PMA
F
mean no. exocytic site number/cell
20
15
10
5
0
unstim
hist
PMA
Control
Bleb
CCE
G
proportion of exocytic sites>2μm²
0.25
0.20
0.15
0.10
0.05
0.00
**
ns
***
ns
histamine
PMA
Control
Bleb
CCE
Control
Bleb
CCE

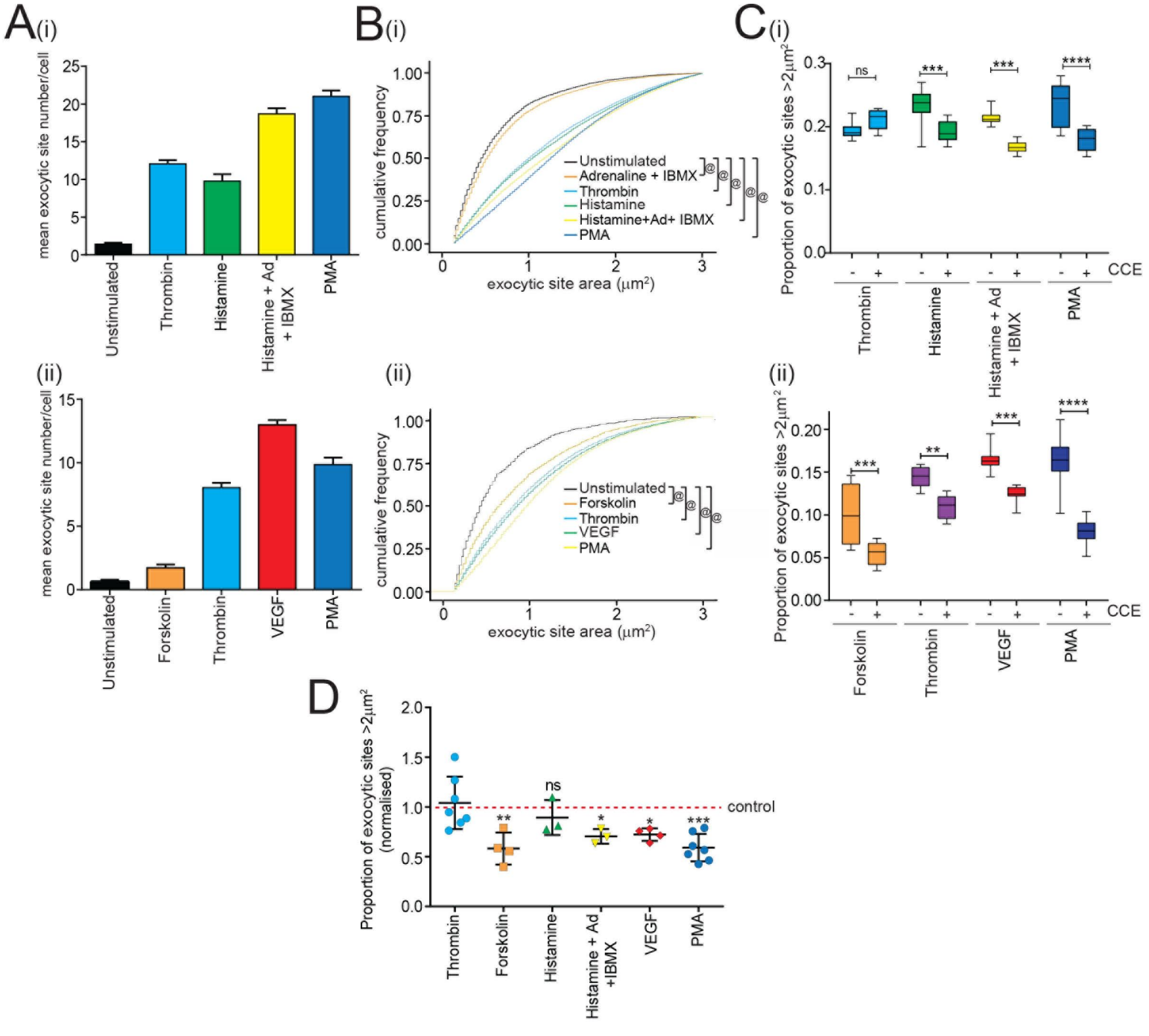
A(i)
mean exocytic site number/cell
Unstimulated
Thrombin
Histamine
Histamine + Ad + IBMX
PMA
(ii)
mean exocytic site number/cell
Unstimulated
Forskolin
Thrombin
VEGF
PMA
B(i)
cumulative frequency
exocytic site area (μm²)
Unstimulated
Adrenaline + IBMX
Thrombin
Histamine
Histamine+Ad+ IBMX
PMA
(ii)
cumulative frequency
exocytic site area (μm²)
Unstimulated
Forskolin
Thrombin
VEGF
PMA
C(i)
Proportion of exocytic sites >2μm²
ns
CCE
Thrombin
Histamine
Histamine + Ad + IBMX
PMA
(ii)
Proportion of exocytic sites >2μm²
CCE
Forskolin
Thrombin
VEGF
PMA
D
Proportion of exocytic sites >2μm² (normalised)
control
Thrombin
Forskolin
Histamine
Histamine + Ad +IBMX
VEGF
PMA

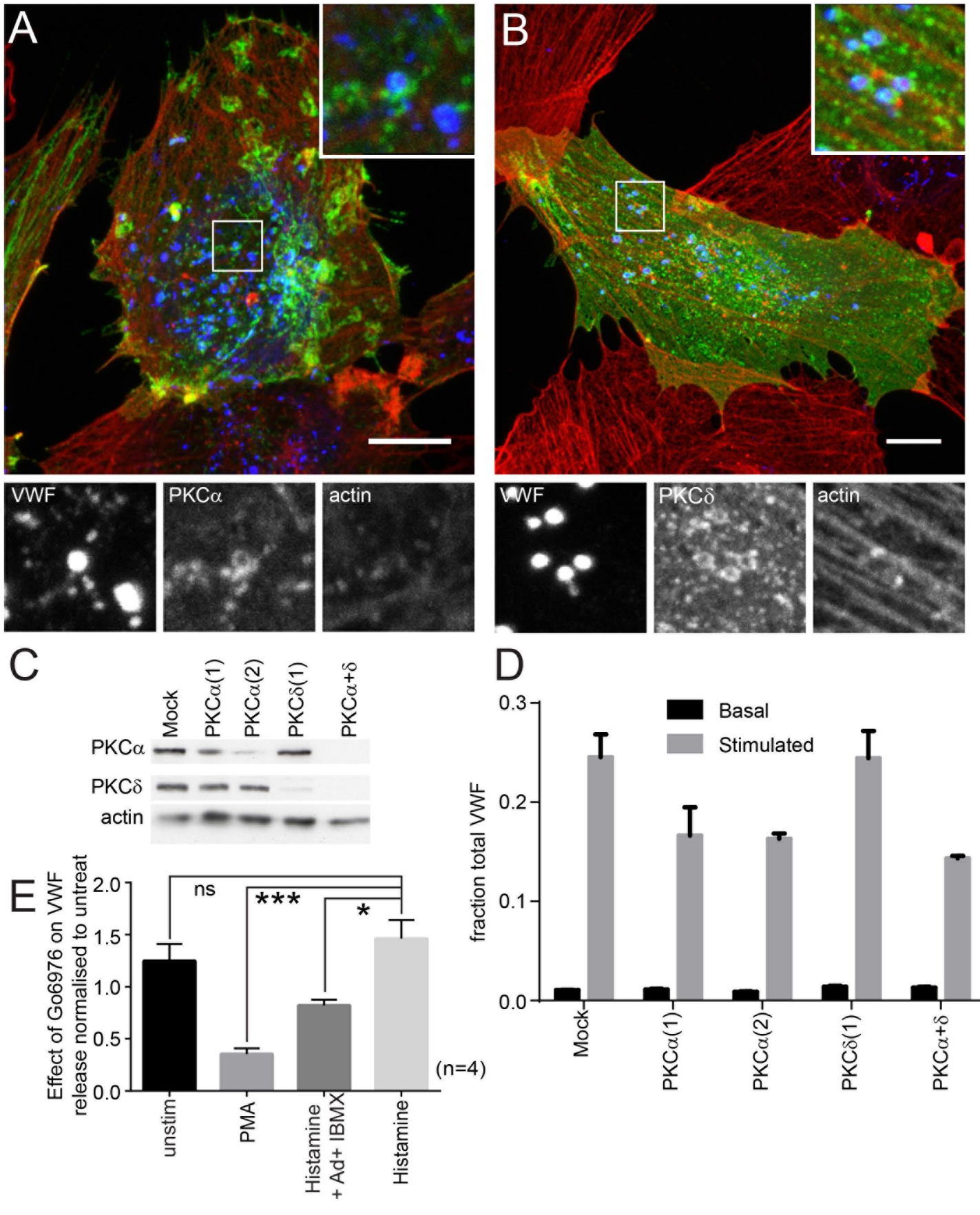
A
B
VWF
PKCα
actin
VWF
PKCδ
actin
C
Mock
PKCα(1)
PKCα(2)
PKCδ(1)
PKCα+δ
PKCα
PKCδ
actin
D
Basal
Stimulated
fraction total VWF
0.3
0.2
0.1
0.0
Mock
PKCα(1)
PKCα(2)
PKCδ(1)
PKCα+δ
E
Effect of Go6976 on VWF release normalised to untreat
2.0
1.5
1.0
0.5
0.0
ns
***
*
(n=4)
unstim
PMA
Histamine + Ad+ IBMX
Histamine

A

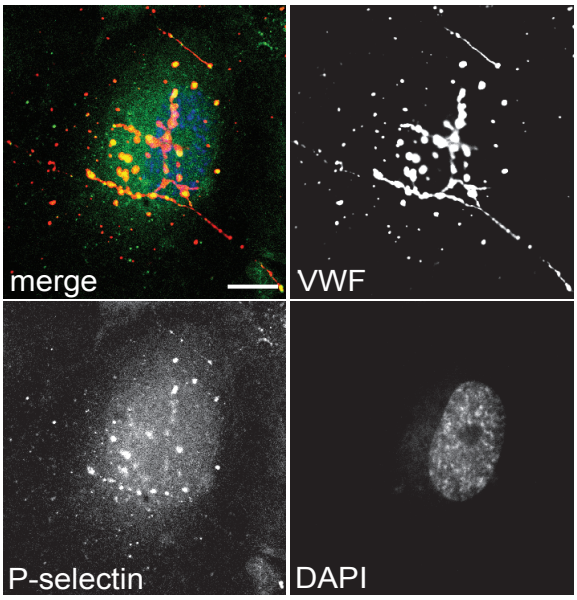

Figure. S1 **P-selectin localisation at exocytosis**
HUVECs were stimulated with 100 ng/ml PMA for 20 min and labelled without permeabilisation for surface VWF (red), P-selectin (green), alongside the nucleus (blue) and imaged on a confocal microscope. Images shown are maximum intensity projections. Bar 10 μm.

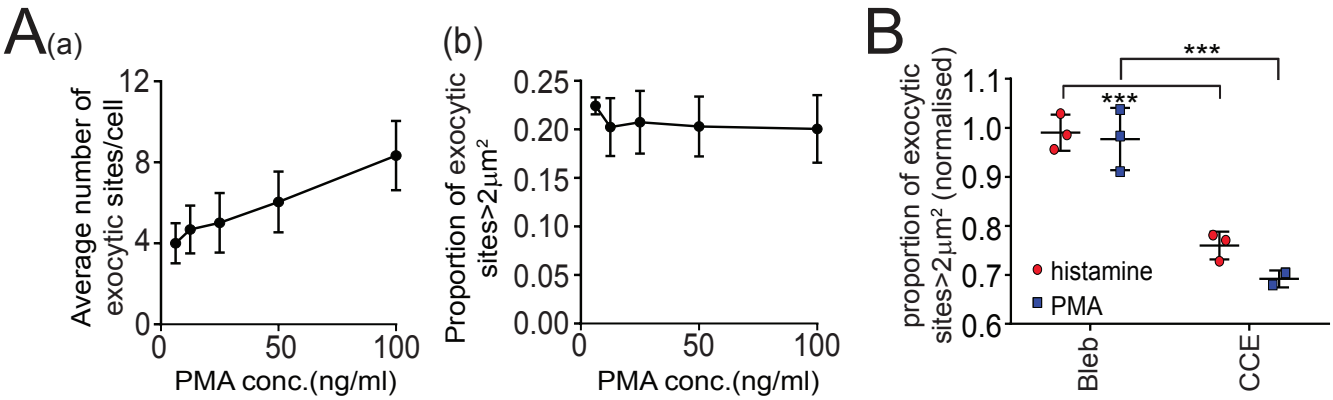

Figure. S2 **High-throughput analysis of exocytic events.**
HUVECs were stimulated with 100ng/ml PMA for 10 minutes, or left unstimulated followed by staining for external VWF, plasma membrane with wheat germ agglutinin (WGA) and the nucleus (DAPI). Images were acquired using the Opera high-content screening (PerkinElmer) confocal microscope. Nine fields of view were acquired per well, and eight wells imaged per condition. External VWF was segmented using a custom-designed program. (A) HUVECs were stimulated with serial dilutions of PMA (100ng/ml – 6.25ng/ml) for 10 minutes and the number and area of segmented external exocytic sites measured. The average number of exocytic sites per cell (Aa) and average proportion of exocytic sites with area greater than 2µm^2 (Ab) is shown. Bar represent SEM (n=4). Statistical significance was assessed using 1-way ANOVA with Tukey's multiple comparison test (Ab) and no significant difference is seen between any concentration of PMA. (B) HUVEC were pre-treated with blebbistatin (25 µM) or CCE (1 µM) for 15 min before stimulation with histamine and PMA. The mean proportion of larger (area greater than 2µm^2) exocytic sites in blebbistatin or CCE-treated cells (derived from the mean of 8 wells per experiment) was normalised to the proportion of large sites in control samples, per experiment (N=3 independent experiments). Statistical significance was assessed with 2-way ANOVA sidak's multiple comparison test , ** P<0.05 and *** P<0.005.

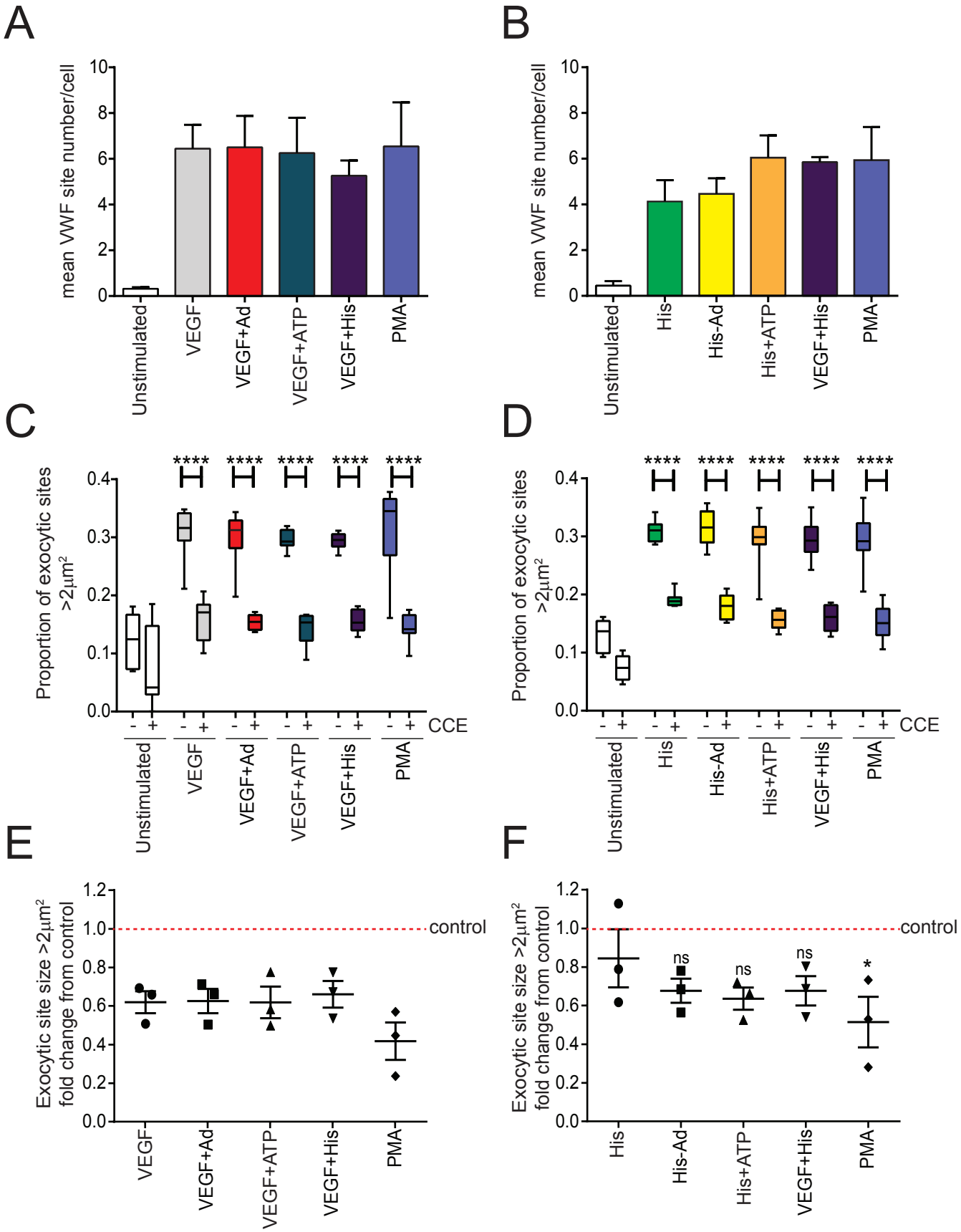

Figure S3. **Analysis of actin ring function with a variety of secretagogues.**
HUVECs were treated with or without 1μM CCE before being stimulated with either 40ng/ml VEGF alone or in combination (A, C, E), 100μM histamine alone or in combination (B, D, F) or 100ng/μl PMA (A-F) for 10 minutes, followed by staining for external VWF and the nucleus. Images were acquired using the Opera high-content screening confocal microscope. Nine fields of view were acquired per well, and eight wells imaged per condition. Representative experiments are shown (A-D) from N=3 (A, C) and N=4 (B, D) independent experiments. (A-B) Mean number of exocytic sites per cell per well with the different secretagogue combinations. Bars represent SEM. (N=8 wells). (C-D) The proportion of VWF sites greater than 2μm² following stimulation with secretagogues alone or in combination and with or without CCE (1μM). Boxes represent 25th-75th percentiles, whiskers represent minimum and maximum values. (N=8 wells). (E-F) The mean proportion of exocytic sites with area greater than 2μm² following stimulation with a number of secretagogues in the presence of CCE normalised to the mean proportion of large sites in control samples. Bars represent SEM. Mean value is derived from the mean of N=8 wells per experiment (E; N=3, F; N=4). Statistical significance was assessed using 2-way ANOVA with Sidak's multiple comparison test (C-D) or 1-way ANOVA with Dunnet's multiple comparisons test (E-F). * P<0.05, **** P<0.0001, ns=not significant.

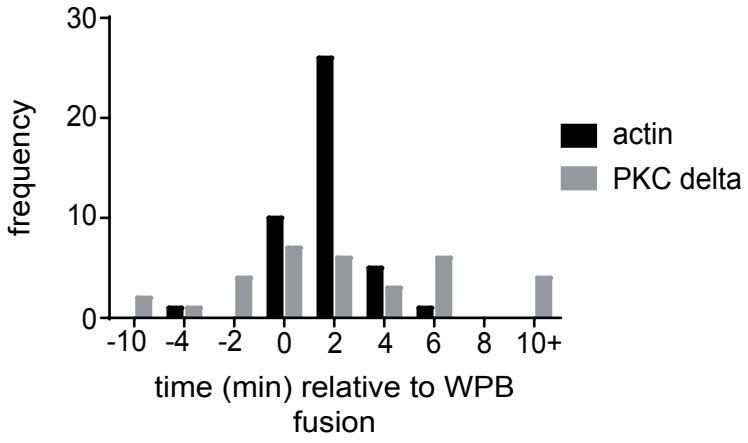

Figure. S4 **The timing of PKC delta recruitment to exocytic sites**
HUVECs were nucleofected with mcherry-Pselectin.lum and PKCdGFP or mcherry-Pselectin.lum and lifeact GFP and imaged with a spinning-disk confocal microscope in the presence of 100 ng/ml PMA (n=9). Z stacks were acquired at a spacing of 0.5 mm every 5 s for 10 min. The timing of actin and PKC delta recruitment was plotted relative to the point of fusion (as determined by the loss of mcherry-Pselectin.lum).

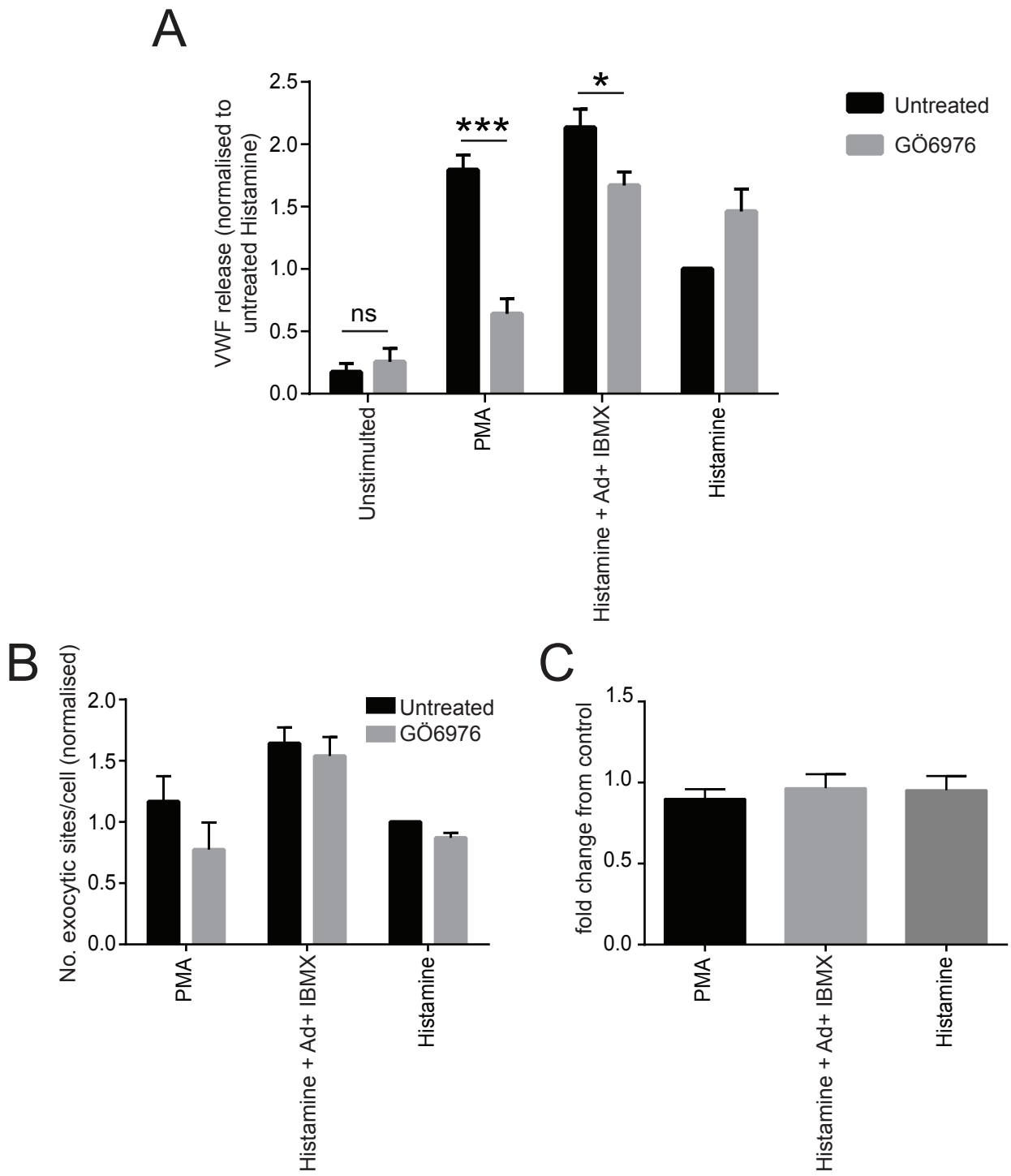

Figure S5. **Effect of GÖ6976 on exocytic site size and number.**
HUVECs were treated with or without 1μM GÖ6976 for 15minutes before being stimulated with 100ng/μl PMA, 100μM Histamine or 100μM Histamine/10μM adrenalin/100μM IBMX for 10-30 minutes. The VWF secretion was determined by ELISA (30 minutes stimulation) (A) or following 10 minutes stimulation, samples were stained for external VWF, wheat germ agglutinin (WGA) to label the plasma membrane with or DAPI to label the nucleus. Images were acquired using the Opera high-content screening (PerkinElmer) confocal microscope. Nine fields of view were acquired per well, and eight wells imaged per condition. Data from a representative experiment is shown (n=4) (B,C). (A) The amount of VWF released is determined relative to cells stimulated with Histamine (B) Mean number of exocytic sites/cell with the different secretagogues in the presence or absence of GÖ6976. (C) The proportion of exocytic sites greater than 2μm^2 with different secretagogues in the presence of GÖ6976 normalised to an untreated control.